Effect of Annealing on the Crystallization and Properties of Electrospun Polylatic Acid and Nylon 6 Fibers

Ah-Ra Cho,[1] Dong Myeong Shin,[1] Hyun Wook Jung,[1] Jae Chun Hyun,[1] Joo Sung Lee,[2] Daehwan Cho,[3] Yong Lak Joo[3]

[1]*Department of Chemical and Biological Engineering, Korea University, Seoul 136-713, Korea*
[2]*LG Chem/Research Park, Daejeon 305-380, Korea*
[3]*School of Chemical and Biomolecular Engineering, Cornell University, Ithaca, New York 14853*

Received 4 December 2009; accepted 6 June 2010
DOI 10.1002/app.33262
Published online 3 November 2010 in Wiley Online Library (wileyonlinelibrary.com).

ABSTRACT: Electrospinning experiments for solutions of two polymers with different crystallization rates, polylatic acid (PLA), and nylon 6 solutions have been carried out. Hexafluoroisopropanol (HFIP) was used as a common solvent to dissolve both PLA and nylon 6. Using the fact that nylon 6 has the faster crystallization rate than PLA, the effect of thermal annealing conditions on the crystal structures of two electrospun fibers has mainly been studied via thermal and mechanical analysis. First, optimal conditions for the formation of uniform nanofibers have been determined by observing their morphology and rheological properties. Thermal analysis revealed that PLA as-spun fiber exhibits cold crystallization due to insufficient crystal growth in spinline. Also, the effect of thermal annealing on the structural change of nylon 6 fibers including the degree of flow-induced crystallization is totally different from that of PLA fibers. Finally, tensile measurements of annealed fibers show that the ultimate tensile strength and Young's modulus gradually increases with increasing annealing time for both PLA and nylon 6 mats, resulting from the further growth of crystal structures. © 2010 Wiley Periodicals, Inc. J Appl Polym Sci 120: 752–758, 2011

Key words: solution electrospinning; annealing; PLA; nylon 6; thermal properties; crystal structure; mechanical properties

INTRODUCTION

Electrospinning technique, incorporating high-electric field for the strong extensional deformation of a spinline jet, has been widely used to produce submicron fibers with high-surface area for its simplicity and versatile application fields such as filtration devices, solar cells, nonwetting textile surfaces, wound dressings, tissue scaffolds, and so on.[1–4] Theoretical analyses on modeling with viscoelastic nature[5–7] and stability related with axisymmetric instability and whipping (or chaotic bending instability)[8–11] in this process have been scrutinized for last two decades. Also, experimental observations on morphology and physical properties of as-spun fibers using solution[12–19] or melt[20,21] electrospinning processes have been so far extensively explored by many researchers in both academia and industry.

To uniformly manufacture electrospun fibers with high quality, it is crucial to keenly understand the relationship between process conditions and properties of polymeric materials to be spun. Final physical properties and structure of electrospun fibers have been profoundly affected by dynamical behavior in spinline governed by strong elongational deformation and crystallization kinetics triggered by its flow strength.[22–24]

In this study, we compare crystal structures of two sub-micron fibers with different crystallization rates via solution electrospinning by altering the thermal annealing time. For example, two polymers adopted here are polylactic acid (PLA) with slow crystallization rate and fast crystallizable nylon 6.[25,26] The former is well-known as one of environmental-friendly biodegradable polymers which is newly emerging in many application fields[15,16] and the latter is a commercial polymer with superior thermal resistance and mechanical properties in comparison with polyolefins.[27,28] PLA possesses a thermodynamically stable α with lamellar-folded chain and meta-stable β crystal with fibril structure which can be formed under highly oriented processing conditions.[21,22,29] As for nylon 6, several crystal structures, e.g., meta-stable γ and mesomorphic β forms which are frequently generated through drawing processing,[30,31] as well as a stable α one, can be observed. Although there have been many reports dealing with the structures inside

Correspondence to: H. W. Jung (hwjung@grtrkr.korea.ac.kr) (or) Y. L. Joo (ylj2@cornell.edu).

Contract grant sponsor: MEST (Mid-Career Researcher Program NRF Grant); contract grant number: R01-2008-000-11701-0.

Contract grant sponsor: Korea University and Seoul R&BD Program.

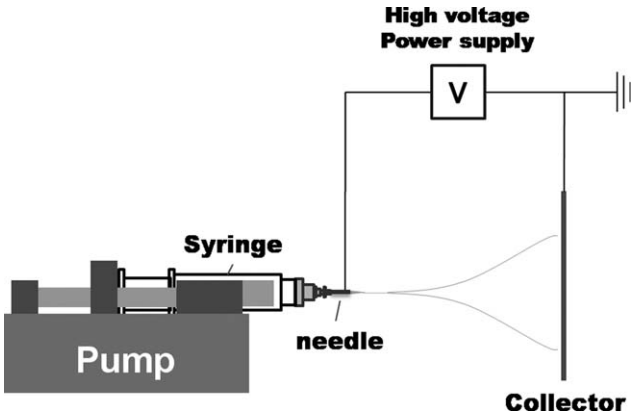

Figure 1 Schematic diagram of electrospinning apparatus.

electrospun fibers, it is uncommon to study the effect of annealing on their structural evolution. Therefore, we have tried to elucidate how the crystal structures of PLA and nylon 6 electrospun fibers develop with annealing time, by comparing their thermal, structural, and mechanical properties.

EXPERIMENTAL

Materials

Polymers used in this study are polylactic acid (PLA, Natureworks 4032D, M_w: 220,000, T_g: 60°C, T_m: 169.5°C) and nylon 6 (Hyosung, M_w: 22,910, T_g: 47°C, T_m: 224.1°C). Before dissolving in the solvent, they were sufficiently dried in vacuum oven (4 and 8 h at 80°C for PLA and nylon 6, respectively). As a common solvent, HFIP (1,1,1,3,3,3,-hexafluora-2-propanol; Aldrich) was selected for easy dissolution of both polymers and its fast evaporation in spinline. Two 13 wt % polymer solutions were finally stirred for 12 h before electrospinning experiment.

Electrospinning apparatus

Electrospinning apparatus consists of three parts as introduced in many other reports: High voltage (up to 30 kV) for using electric field between needle and collector, syringe pump (PHD 22-2000, Harvard Apparatus), and aluminum plate collector for receiving as-spun fibers (Fig. 1). Experiment was performed at about 25°C and 41.5% relative humidity. By changing applied voltage, spinline length, and flow rate, optimal processing conditions for uniform fibers have been determined. All as-spun fibers were directly kept in vacuum oven at room temperature for 24 h to minimize the possibility of residual solvent within fibers and perform ensuing experimental tests.

Annealing

Electrospun fibers were thermally annealed at 80°C for PLA and 180°C for nylon 6 between their glass transition and melting temperatures for 1, 3, and 6 h in vacuum oven, respectively, considering their thermal degradation and mobility. It is noted that a little shrinkage of PLA fibers is observed after 6-h annealing. Nylon 6 as-spun fibers showed insignificant effect of annealing on the change of crystal structure under 160°C for 6 h and also a little thermal degradation after 6-h annealing at 205°C.[30]

Characterization

Various properties of as-spun annealed fibers were measured as follows. Rheological properties of two polymer solutions such as shear viscosity and storage/loss moduli were acquired from rate-sweep and frequency-sweep modes of AR2000. Morphologies of electrospun fibers have been captured from FE-SEM (field emission scanning electron microscope; Hitachi S-4300). Their thermal properties have been obtained from DSC (Perkin-Elmer Differential Scanning Calorimeter7) with heating rate 10°C/min. XRD (Rigaku Co., D/Max-2500/PC) has been incorporated to observe the crystal structural properties of the samples under 40 mA and 200 kV conditions, using Cu target. The scanning rate was 0.3°/min in 20–40° range of 2θ. Finally, according to the ASTM D638, the uniaxial tensile strength of 20 mm × 20 mm rectangular nonwoven mats has been recorded with 10 mm/min cross-head speed of a universal testing machine (Instron 5566).

RESULTS AND DISCUSSION

Rheological properties of polymer solutions

Both PLA and nylon 6 polymer in HFIP solutions basically exhibit Newtonian behavior. The viscosity of PLA solution was higher than that of nylon 6 solution as displayed in Figure 2(a). Also, elastic (G') and viscous (G'') moduli of PLA solution are greater than those of nylon 6 case [Fig. 2(b)]. From the G' and G'' data, the single relaxation times of PLA and nylon 6 solutions are found to 0.004 s and 0.0028 s, respectively, implying that PLA solution is slightly more viscoelastic in comparison with nylon 6 case. Although the extensional viscosity of electrospinning solutions have been measured previously using conventional extensional rheometer such as capillary breakup extensional rheometer (CaBER), measuring extensional rheological properties of current polymer solutions will be extremely difficult because of the fast evaporation rate of HFIP solvent.[32]

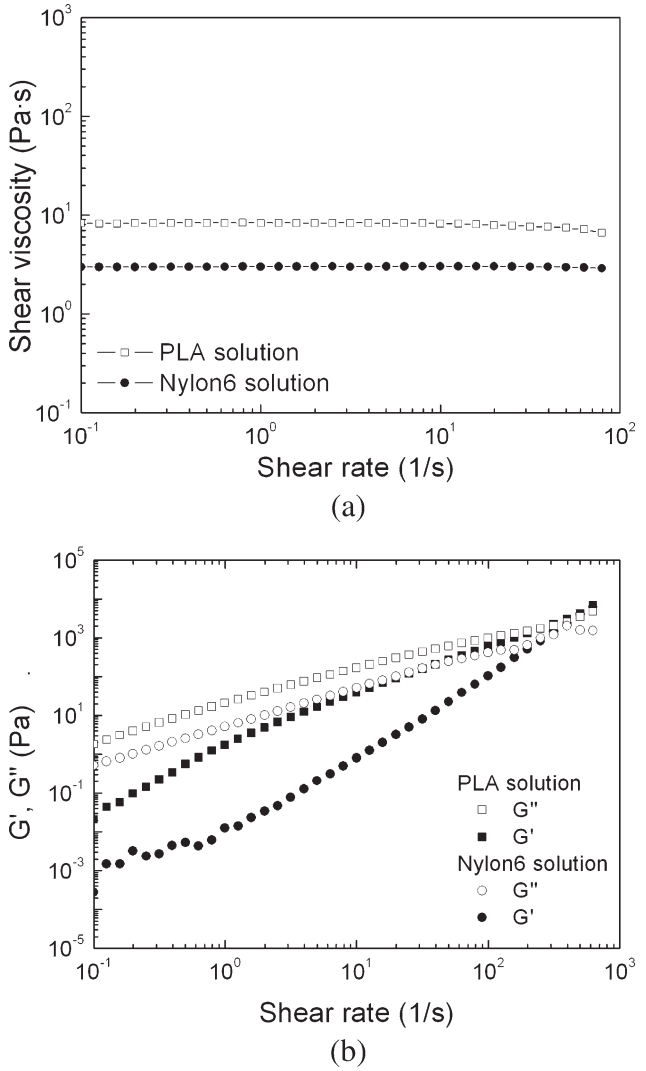

Figure 2 (a) Shear viscosities and (b) storage and loss moduli of PLA and nylon 6 in HFIP solutions.

Fabrication of PLA and nylon 6 electrospun fibers

One possible standard process condition for producing uniform fibers with less than 2 μm diameter from both PLA and nylon 6 solutions has been chosen as follows by observing their morphology: electric voltage (15 kV), flow rate (1.5 mL/h), spinline distance (23 cm), and needle or spinneret diameter (417 μm). Above condition set has been applied to thoroughly compare their structural variations along with the annealing time. It has been found that the fiber morphology is almost same over 15 cm spinline length [Fig. 3(a,b)] enough to almost evaporate HFIP solvent in spinline under the given conditions (We adjusted the spinline distance to somewhat lengthy 23 cm for guaranteeing the PLA and nylon 6 fibers with little or no solvent despite the fast evaporating characteristic of HFIP, and carefully kept and dried them in vacuum oven at room temperature.). It can be also substantiated that high voltage to be applied makes the fiber diameter a little larger [Fig. 3(c)], inducing shorter residence time to be deformed in spinline and not severe whipping phenomenon in comparison with the standard case, even though it can alter the deformation rate in spinline. Thus, it has proved that aforementioned process condition is suitable for manufacturing uniform electrospun PLA and nylon 6 fibers from the comparative observation of fiber morphology. It is worth noting that nylon 6 fiber was thinner than PLA one due to the low-viscous nature of nylon 6 solutions [Fig. 3(d)].

Thermal analysis of annealed PLA and nylon 6 fibers

Figure 4 shows DSC thermograms of PLA bulk resin and fibers annealed at 80°C. Interestingly, cold crystallization peak is observed in as-spun and shortly annealed fibers, as reported in Zhou et al.,[21] representing that the crystallization in these cases is further developed at initial heating stage through DSC analysis. This phenomenon is caused by the insufficient crystal growth inside PLA as-spun fibers with short residence time and relatively slow crystallization rate in uniaxial spinning flow regime. As the annealing time thenceforth increases, in other words, as adequate heat energy is supplied into as-spun fibers before DSC measurement, cold crystallization peak disappears and both melting temperature and crystallinity in fibers are raised (Table I). It is noticed that new β crystal is found in electrospun fibers with increasing annealing time [Fig. 4(b)], as will also be explained in the following section.

On the other hand, nylon 6 as-spun fiber does not exhibit cold crystallization due to its fast crystallization characteristic in contrast to PLA (Fig. 5). However, Liu et al.[18] reported cold crystallization behavior of as-spun fibers from their DSC measurement. It is thought that this discrepancy might be ascribed by moderately different process conditions. Also, it can be observed that two distinct melting peaks in as-spun fibers near the melting temperature region, not showing in the bulk resin, are steadily broadening with the evolution of annealing time, judging from that γ crystal structure in fibers dominantly grows during the annealing. Degree of crystallization predicted from this analysis is surely raised with annealing time, as similarly in the PLA case. However, melting temperature of nylon 6 is somewhat decreased as annealing time rises, affected by dominant γ form in electrospun fibers.[30,33]

Structural analysis of annealed PLA and nylon 6 fibers

XRD peaks of annealed PLA fibers have been compared, including that of the bulk resin in Figure 6(a).

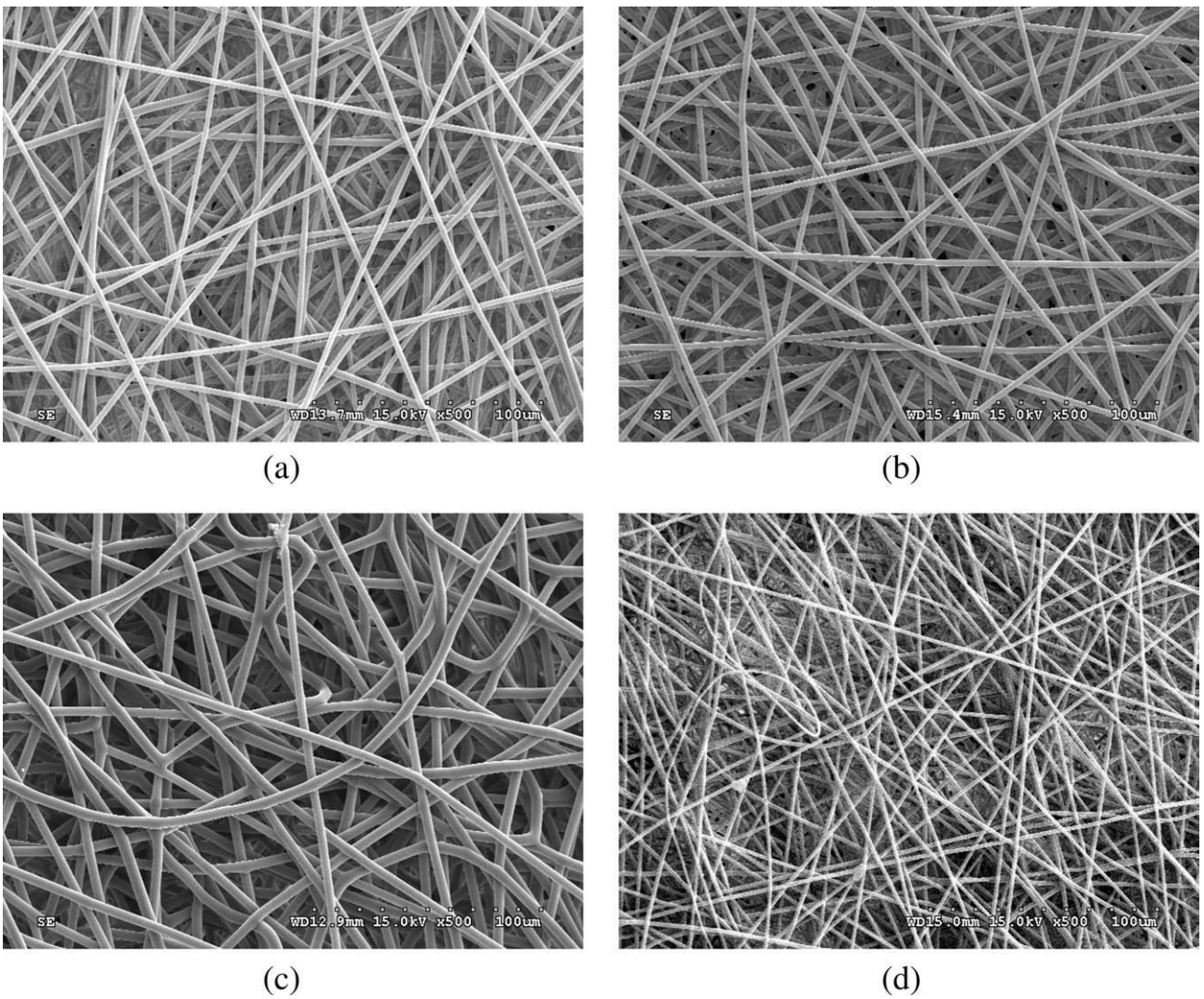

Figure 3 Morphology of PLA as-spun fiber at (a) 15 cm and (b) 23 cm spinline distance (15 kV, 1.5 mL/h), and at (c) 25 kV applied voltage (23 cm, 1.5 mL/h). (d) Morphology of nylon 6 as-spun fiber at 23 cm spinline distance (15 kV, 1.5 mL/h).

From the XRD peak of PLA as-spun fiber, it has been corroborated that the amorphous phase is dominant in it because there is not enough time for the crystal growth in spinline. However, the crystal structure has been developed by annealing treatment, offering sufficient heat energy for the crystal growth. For instance, thermodynamically stable α crystal form can be noticeably observed at 16.33° with sharp and narrow peak. *d*-Spacing calculated from Bragg equation, $n\lambda = 2d \sin\theta$, is about 0.54 nm at this point. This form also exists at 18.6° of 2θ with 0.48 nm of *d*-spacing. β crystal structure resulting from the high-extensional deformation in spinline is also generated at 26.50° and 27.88° with 0.34 nm and 0.32 nm of *d*-spacing, respectively. As illustrated in Figure 6(b), relative ratios of amorphous and crystalline phases at some dominant peaks have been estimated from XRD data for PLA bulk resin and annealed fibers. As the annealing time rises, two leading α crystalline phases have grown from the incipient amorphous-dominant phase in as-spun fibers, and finally approached toward values of the resin state.

In the case of nylon 6 as-spun fibers [Fig. 7(a)], there exists some portion of crystal structure in as-spun fiber due to its fast crystallization feature and also flow-induced crystallization effect acting on the spinline[24] in contrast to PLA case, albeit it was not annealed. As the annealing time increases at 180°C, the crystal structure in nylon 6 fibers is of course further grown. α structures are mainly found at 20.00° with 0.44 nm and 25.05° with 0.36 nm. Also, the γ and β structures are observed at 21.19° with 0.42 nm and 37.2° with 0.24 nm, respectively.[17,34] Especially, γ crystal is strikingly developed with increasing annealing time [Fig. 7(b)], demonstrating the distinct difference from the PLA case. The crystal structure of nylon 6 as-spun fiber is restored into its resin state with dominant portion of α crystal, when both bulk resin and as-spun fibers are melted over melting temperature, as revealed in Figure 7(c), convincing that the

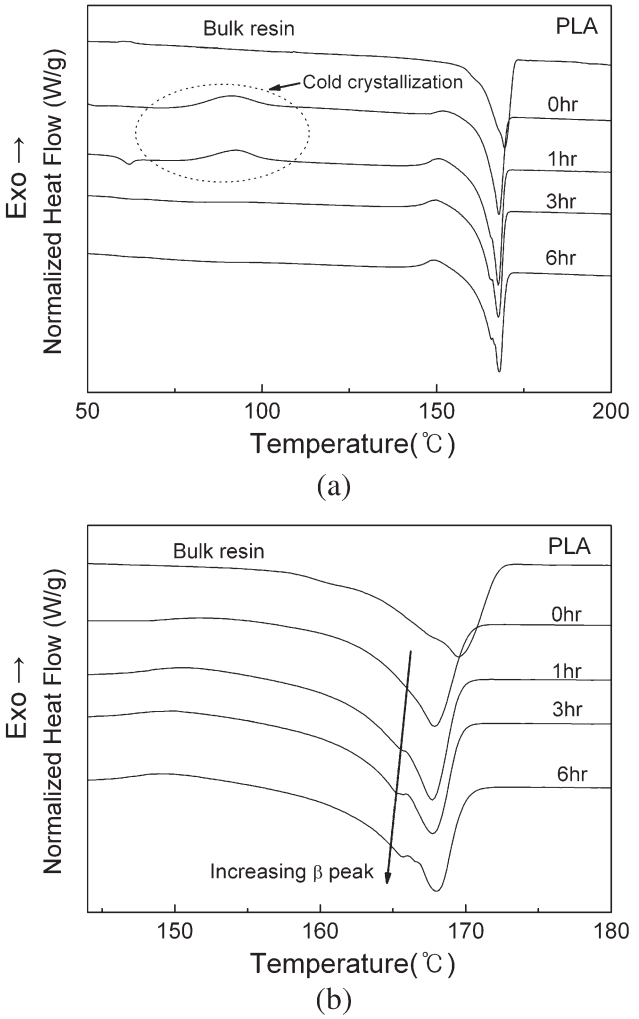

Figure 4 (a) DSC thermograms of PLA bulk resin and as-spun fiber annealed at 80°C and (b) magnification of crystalline melting peaks.

growth of γ crystal in nylon 6 fibers under as-spun or annealed state, not α form in the conventional bulk resin state, is attributed to highly oriented extensional deformation imposed in spinline.

Mechanical analysis of annealed PLA and nylon 6 mats

The averaged Young's modulus and ultimate tensile strength for annealed PLA and nylon 6 mats

TABLE I
Crystallinity and Melting Temperature of Annealed PLA and Nylon 6 As-Spun Fibers from DSC Measurement

		Annealing time (h) of electrospun fibers			
		0	1	3	6
Degree of crystallinity (%)	PLA	20.7	27.5	35.6	36.1
	Nylon 6	30.0	35.8	36.7	36.4
T_m (°C)	PLA	167.9	167.7	167.7	168.1
	Nylon 6	221.7	219.7	219.5	218.5

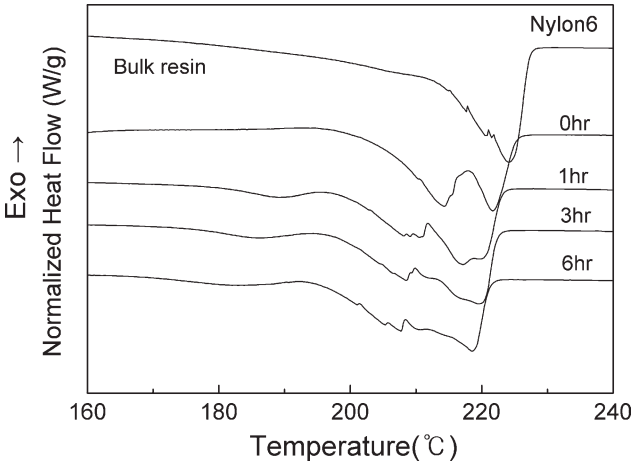

Figure 5 DSC thermograms of nylon 6 bulk resin and as-spun fiber annealed at 180°C.

entangled with nonwoven fibers have been finally measured using UTM (Fig. 8). As annealing time rises, the ultimate tensile strength and Young's

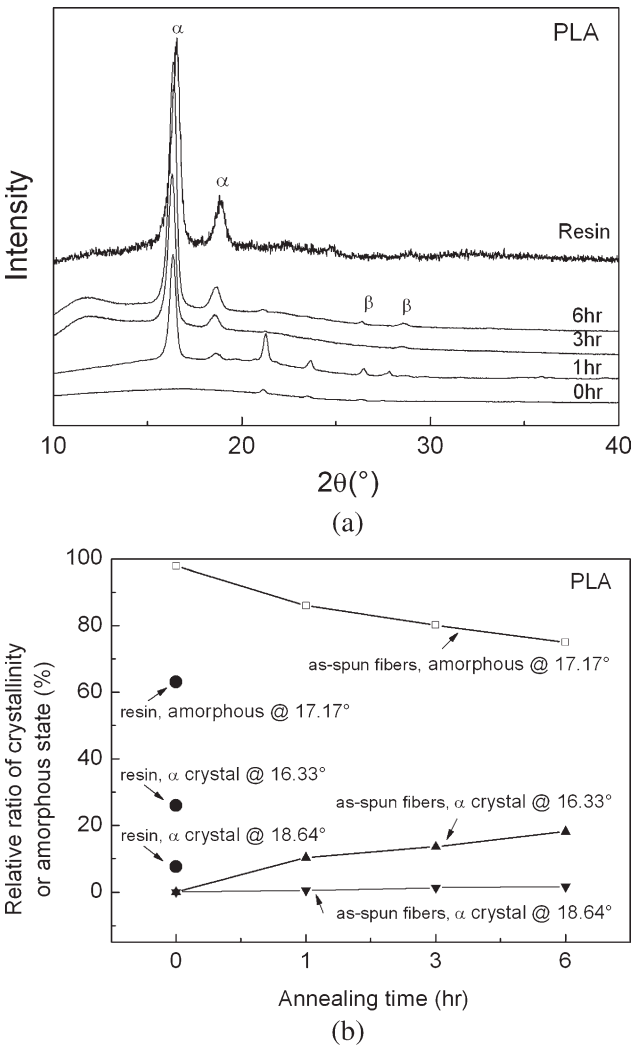

Figure 6 (a) XRD peaks and (b) relative crystallinity or amorphous state ratio of PLA bulk resin and as-spun fiber annealed at 80°C.

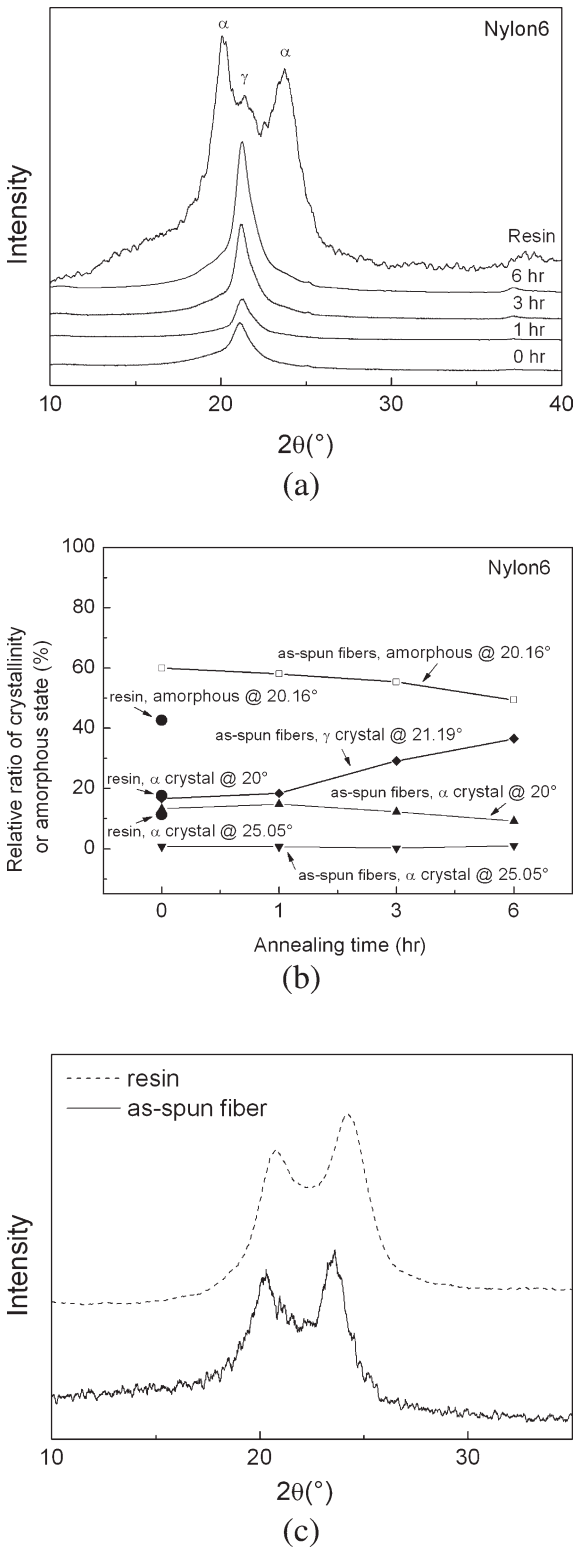

Figure 7 (a) XRD peaks, (b) relative crystallinity or amorphous state ratio of nylon 6 bulk resin and as-spun fiber annealed at 180°C, and (c) XRD peaks of nylon 6 bulk resin and as-spun fiber melted at 240°C for 10 min.

modulus gradually rises for both PLA[35] and nylon 6[28,36] mats, resulting from the further growth of crystal structures. It has been recognized from the data that ultimate tensile strength for annealed nylon 6 fibers is higher than that for PLA case, but Young's modulus for nylon 6 is lower than that for PLA.

CONCLUSIONS

Properties and structures of PLA and nylon 6 fibers via solution electrospinning process have been experimentally investigated by changing annealing time. Morphological, thermal, structural, and mechanical analyses have been incorporated to exhibit the evolution of the crystal structures in both electrospun fibers with annealing, considering ambivalent aspects of the spinline regime for the crystal formation, i.e., crystallization kinetics induced by the high-extensional deformation in spinline and residence time for a fluid jet to travel the spinline. It has been

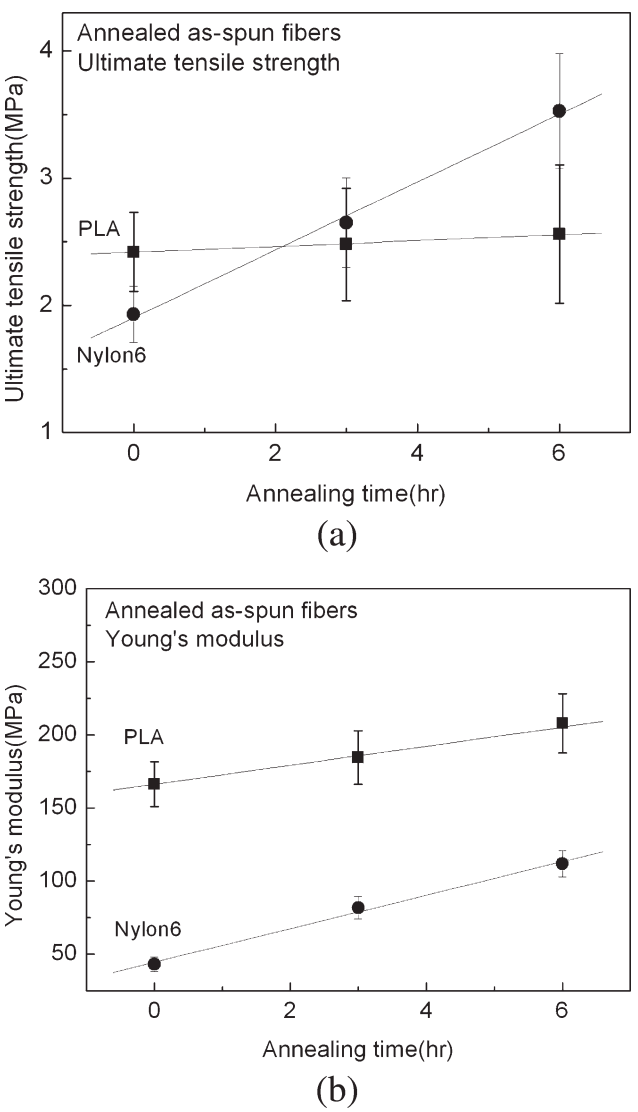

Figure 8 (a) Ultimate tensile strength and (b) Young's modulus of PLA and nylon 6 electrospun mats.

revealed that PLA as-spun fiber with slow crystallization rate shows cold crystallization in DSC thermograms and its large portion of amorphous phase further evolves toward the original crystalline phase of PLA bulk resin as annealing time rises. Meanwhile, in the nylon 6 case with fast crystallization rate, γ crystal structure, which is a distinct flow-induced crystal in spinline, is formed in as-spun fibers and also this increasingly grows as annealing time increases, not toward the resin state.

References

1. Reneker, D. H.; Yarin, A. L. Polymer 2008, 49, 2387.
2. Huang, Z. M.; Zhang, Y. Z.; Kotaki, M.; Ramakrishna, S. Compos Sci Technol 2003, 63, 2223.
3. Subbiah, T.; Bhat, G. S.; Tock, R. W.; Parameswaran, S.; Ramkumar, S. S. J Appl Polym Sci 2005, 96, 557.
4. Doshi, J.; Reneker, D. H. J Electrostat 1995, 35, 151.
5. Carroll, C. P.; Joo, Y. L. Phys Fluids 2006, 18, 053102–1.
6. Feng, J. J. Phys Fluids 2002, 14, 3912.
7. Feng, J. J. J Non-Newtonian Fluid Mech 2003, 116, 55.
8. Carroll, C. P.; Joo, Y. L. J Non-Newtonian Fluid Mech 2008, 153, 130.
9. Yarin, A. L.; Koombhongse, S.; Reneker, D. H. J Appl Phys 2001, 90, 4836.
10. Hohman, M. M.; Shin, M.; Rutledge, G.; Brenner, M. P. Phys Fluids 2001, 13, 2201.
11. Shin, Y. M.; Hohman, M. M.; Brenner, M. P.; Rutledge, G. C. Appl Phys Lett 2001, 78, 1149.
12. Ma, Z.; Kotaki, M.; Yong, T.; He, W.; Ramakrishna, S. Biomaterials 2005, 26, 2527.
13. Reneker, D. H.; Fong, H. Polymeric Nanofibers, ACS Symposium Series 918, American Chemical Society, Washington DC; 2006.
14. Buchko, C. J.; Kozloff, K. M.; Martin D. C. Biomaterials 2001, 22, 1289.
15. Kim, K.; Yu, M.; Zong, X. H.; Chiu, J.; Fang, D. F.; Seo, Y. S.; Hsiao, B. S.; Chu, B.; Hadjiargyrou, M. Biomaterials 2003, 24, 4977.
16. Blackwood, K. A.; McKean, R.; Canton, I.; Freeman, C. O.; Franklin, K. L.; Cole, D.; Brook, I.; Farthing, P.; Rimmer, S.; Haycock, J. W.; Ryan, A. J.; MacNeil, S. Biomaterials 2008, 29, 3091.
17. Jose, M. V.; Steinert, B. W.; Thomas, V.; Dean, D. R.; Abdalla, M. A.; Price, G.; Janowski, G. M. Polymer 2007, 48, 1096.
18. Liu, Y.; Cui, L.; Guan, F.; Gao, Y.; Hedin, N. E.; Zhu, L.; Fong, H. Macromolecules 2007, 40, 6283.
19. Fong, H., Liu, W.; Wang, C. S.; Vaia, R. A. Polymer 2002, 43, 775.
20. Lyons, J.; Li, C.; Ko, F. Polymer 2004, 45, 7597.
21. Zhou, H.; Green, T. B.; Joo, Y. L. Polymer 2006, 47, 7497.
22. Hoogsteen, W.; Postema, A. R.; Pennings, A. J.; Brinke, G. T.; Zugenmaier, P. Macromolecules 1990, 23, 634.
23. Samon, J. M.; Schultz, J. M.; Wu, J.; Hsiao, B.; Yeh, F.; Kolb, R. J Polym Sci Part B: Polym Phys 1999, 37, 1277.
24. Zhmayev, E.; Cho, D.; Joo, Y. L. Polymer 2010, 51, 274.
25. Chu, M. J.; Wu, T. M. In Proceedings of the 13th International Conference on Experimental Mechanics, Alexandroupolis, Greece, July 1–6, 2007; p 827.
26. Huang, J. W.; Chang, C. C.; Kang, C. C.; Yeh, M. Y. Thermochim Acta 2008, 468, 66.
27. Li, Y.; Huang, Z.; Lu, Y. Eur Polym J 2006, 42, 1696.
28. Carrizales, C.; Pelfrey, S.; Rincon, R.; Eubanks, T. M.; Kuang, A.; McClure, M. J.; Bowlin, G. L.; Macossay, J. Polym Adv Technol 2008, 19, 124.
29. Sawai, D.; Takahashi, K.; Imamura, T.; Nakamura, K.; Kanamoto, T.; Hyon, S. H. J Polym Sci Part B: Polym Phys 2002, 40, 95.
30. Cho, D.; Zhmayev, E.; Joo, Y. L. Macromolecules, submitted.
31. Seguela, R. J Macromol Sci Polym Rev 2005, 45, 263.
32. Theron, S. A.; Zussman, E.; Yarin, A. L. Polymer 2004, 45, 2017.
33. Kwak, S.-Y.; Kim, J. H.; Kim, S. Y.; Jeong, H. G.; Kwon, I. H. J Polym Sci Part B: Polym Phys 2000, 38, 1285.
34. Auriemma, F.; Petraccone, V.; Parravicini, L.; Corradini, P. Macromolecules 1997, 30, 7554.
35. McCullen, S. D.; Stano, K. L.; Stevens, D. R.; Roberts, W. A.; Monteiro-Riviere, N. A.; Clarke, L. I.; Gorga, R. E. J Appl Polym Sci 2007, 105, 1668.
36. Zussman, E.; Burman, M.; Yarin, A. L.; Khalfin, R.; Cohen, Y. J Polym Sci Part B: Polym Phys 2006, 44, 1482.